Cross, T., De Luca, F., & De Risi, R. (2020). *An experimental comparison of micro-modelling and meso-modelling for an unreinforced masonry wall*. Paper presented at 17th World Conference on Earthquake Engineering, Sendai, Japan.

Peer reviewed version




*17th World Conference on Earthquake Engineering, 17WCEE*
*Sendai, Japan - September 13th to 18th 2020*

# AN EXPERIMENTAL COMPARISON OF MICRO-MODELLING AND MESO-MODEILLING FOR AN UNRIENFOCED MASONRY WALL

T. Cross[1], F. De Luca[2], R. De Risi[3]

[1] *PhD Candidate, University of Bristol, ted.cross@bristol.ac.uk*
[2] *Senior Lecturer, University of Bristol, flavia.deluca@bristol.ac.uk*
[2] *Lecturer, University of Bristol, raffaele.derisi@bristol.ac.uk*

## *Abstract*

The shear response of an unreinforced masonry (URM) wall is assessed using simplified micro-modelling and meso-modelling. The results are then compared to experimental data. Masonry is a highly non-linear material which exhibits high levels of damage, this can make it particularly complex to accurately model for analysis and design purposes. Micro-modelling is the most computationally demanding method of modelling masonry as the brick units and the mortar are individually modelled. Micro-modelling also requires the highest number of material properties. Meso-modelling is less computationally demanding as it models the masonry as a continuum. Meso-modelling requires fewer material properties and they can be obtained from tests on masonry prisms and wallettes. A micro and meso-models are implemented into OpenSees using the "Scientific Toolkit for OpenSees" (STKO) and the materials are modelled using the tension and compression damage model (TC3D) available in STKO. The material parameters are obtained from the experimental study considered as case study herein, where possible, and are otherwise obtained from literature where tests have been carried out on similar materials. The force-displacement curve and the failure mechanism are used as points of comparison with the experimental data. The material properties are then adjusted within their variability as to allow the micro and meso model get better matching with the experimental results. The micro-model does not show similar pushover results with respect to the experimental data and the failure mechanism is different. The micro-model fails in sliding shear and the experimental fails due to diagonal shear cracking. The meso-model better matches the pushover of the experimental test with the peak load being within 10% of the experimental data. It is also observed that failure mechanism for the meso-model is the same as the experimental tests.

*Keywords: Masonry, Meso-modelling, Micro-modelling, OpenSees, STKO*

 



## 1. Introduction

Masonry has been used in construction for over 10,000 years and is still used today throughout the world. The vast majority of construction before the 19th century was formed of masonry and still 30%-50% of new housing construction is formed of masonry. This highlights the importance of accurate and reliable methods for modelling the response of masonry structures to seismic loading, allowing more robust designs and retrofit for existing structures [1].

Masonry is highly non-linear and exhibits high levels of residual damage, causing it to be mathematically complex, to accurately model its structural response to vertical and horizontal loading. Performance based earthquake engineering has led to an increase demand of accurate modelling methods to be used in static pushover and nonlinear dynamic analysis. There are three general methods for modelling masonry with each one having many variations, these are equivalent frame method, meso-modelling and micro-modelling. In literature several attempts have been made to calibrate these modelling techniques to experimental data (e.g., [2][3]).

Micro-modelling is the most computationally demanding and requires detailed material properties as it individually models the bricks, the mortar and the interaction between the two of them. Micro-modelling can then be further broken down into detailed micro-models and simplified micro-models. The main difference between these two models is that the simplified micro-model does not account for the effect of mortar/brick interface [4] as can be seen in Figure 1.

Meso-modelling is a method of modelling unreinforced masonry (URM) as a continuum. It is less computationally heavy than micro-modelling but can be hard to implement on complex geometry and requires calibration of parameters from experimental tests on the masonry rather than simpler testing on the components of the URM [5]. It also needs fewer material properties and these properties are typically obtained from testing of masonry prisms and wallettes.

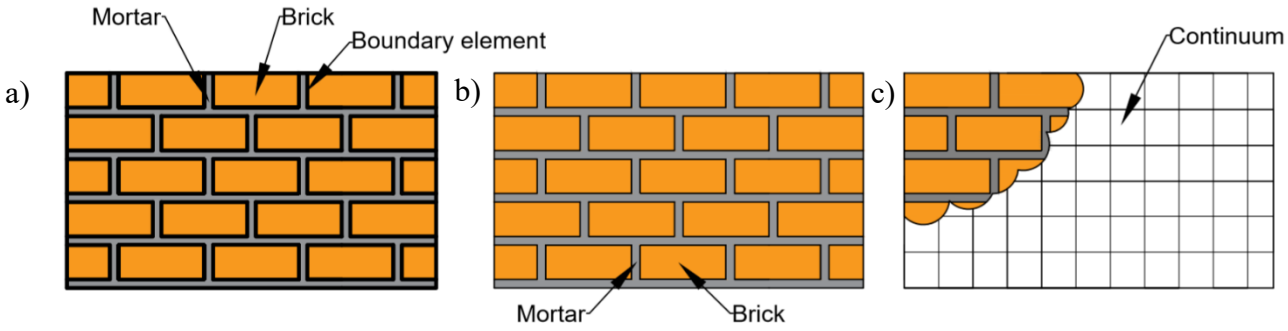


Figure 1. Modelling techniques for masonry walls: a) detailed micro-modelling b) simplified micro-model c) meso-model

This paper compares the results of various masonry modelling techniques with the results of experimental work carried out by the Advanced Construction Technology Center (ACTC), University of Illinois [6]. The primary aim of this work is to investigate the in-plane lateral strength and behavior of unreinforced masonry walls. A single test with a significant damage redistribution is considered to benchmark different modelling approaches implemented in OpenSees using the "Scientific Toolkit for OpenSees" (STKO) and to assess the suitability of simplified micro-modelling and meso-modelling to replicate the experimental test considered.

## 2. Experimental results

The experimental campaign considered is aimed at assessing the effect of the length-to-height ratio by performing the tests on three walls of varying lengths. In this study, only one of these experiments is considered for the assessment with different modelling strategies. The single experimental test selected, is the one referred



 



to as the largest wall and is characterized by a failure mechanism that involves a significant damage redistribution, typically difficult to model through Finite Element (FE) modelling approaches that are generally capable of capturing the initial elastic and generally brittle behavior of URM.

Figure 2 shows this wall and its dimensions, it is formed of solid reclaimed bricks measuring 7.8'' by 3.5'' by 2.2'' (198mm × 89mm × 56mm). An American bond pattern was used with the mortar being 3/8'' (9.5 mm) in thickness and having a cement to sand ratio of 1:6. This was supported by a concrete foundation pad that measures 14' by 5' by 18'' (4267mm × 1524 mm x 457 mm) also depicted in Figure 2. Vertical hydraulic jacks were used to apply a vertical stress of 75 psi (0.52 MPa) and two 110-kip (490 kN) servo-hydraulic actuators were used to apply a lateral load. The mortar is representative of mortars in historic (US) masonry structures, but it can also be representative of typical weak mortars used in developing countries (e.g., [7], [8]).

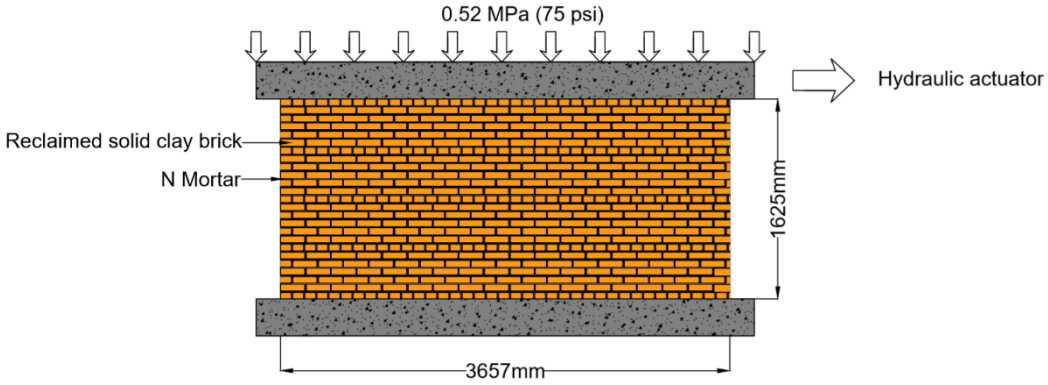


Figure 2. Test rig of masonry wall including concrete foundations and loading beam

This study provided limited details of the material properties used and this provided with the opportunity for a blind calibration of most of the parameters needed for FE modelling and to replicate typical assessment situations of existing URM buildings in which most parameters needed for modelling are not available.
The bricks are described as "solid reclaimed bricks", the study does not explicitly state whether they are fired clay, but this is assumed as they are said to be typical of bricks from the first half of the 20th century. Several ASTM tests were carried out on the bricks to find an average compressive strength of 3480 psi (23.99 MPa). Universal compression tests were carried out on prisms of masonry formed of five bricks. This test was carried out on three types of mortar and three prisms were formed for each mortar type. This test found a compressive strength of 801 psi (5.52 kN) for type N mortar (1:6 cement to sand ratio), which is the type of mortar used in the lateral tests of the wall shown in Figure 2.

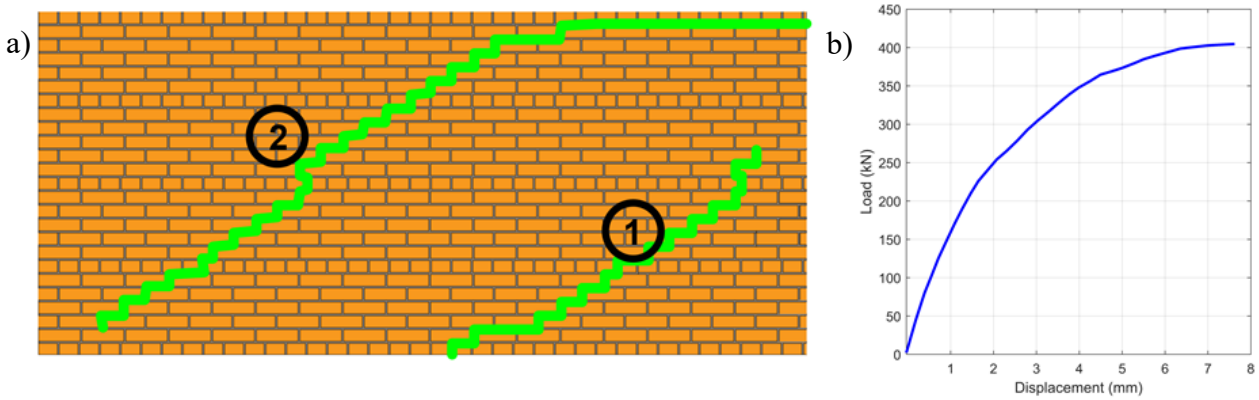


Figure 3. Results of experimental tests (a) cracking sequence of masonry wall (b) lateral load displacement.



 

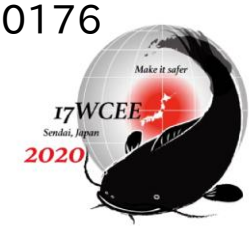



The masonry specimen was subject to four loading cycles however this paper uses the first quarter of a cycle as a point of comparison for the first monotonic loading. This assumption eliminates the effect of strength degradation due to damage. The lateral displacement was measured at the top of the specimen and is shown in Figure 3b. The sequence of cracking was also recorded this is shown on Figure 3a. This specimen underwent diagonal shear cracking, with the crack marked with a (1) appearing at 62% of the ultimate load. Following this a second larger crack, indicated with (2) in Figure 3a, which formed at the peak lateral strength.

## 3 Micro-modelling

Micro-modelling requires individual material properties for both the brick units and for the mortar. As few specific brick parameters are presented with the experimental data, other experimental results must be retrieved from literature. It is stated that the bricks used are 7.8'' long by 3.5'' wide by 2.2'' high (198mm × 89mm × 56mm) and that they are solid. It is also stated that the bricks are representative of typical brick from the first half of this century, this led to the assumption they are made of clay [6]. A uniaxial compression test was carried out on the bricks to find a peak compression strength of 3480 MPa (23.99 MPa). This is the only material property provided for the brick. An in-place flap-jack test is carried out on the mortar indicating that it had a tensile strength of 0.68 MPa.

The micro-modelling of the masonry wall is implemented into OpenSees using the "Scientific Toolkit for OpenSees" (STKO) developed by ASDEA Software Technology. The materials were modelled using a tension and compression damage model (TC3D) developed by Petracca and Camata [9].

First, a blind test is performed to model the experimental response. In this blind test, the parameters are not modified based on the level of matching with the experimental data. Since not all properties necessary for the implementation of the FE model are provided, the necessary properties are retrieved form literature studies on URM material similar to that used in the experimental campaign. As a main source of reference for integrative material properties, a study by Kaushik et al. [10] is considered as it refers to mortar with similar cement to sand ratio (1:6).

Kaushik et al. compares different types of mortar in their study but only the results for 1:6 mortar are considered. While most of parameters necessary for implementation of a simplified micro-model are obtained from Kaushik et al., the tensile strength of bricks has been retrieved from a study by Lourenco et al. [14]. This study is considered pertinent for the experimental study considered as it tests mortar of the same cement sand ratio, tests similar bricks and the peak strength of the bricks have values of 20.8 MPa and 23.99MPa, respectively, being acceptably similar.

Table 1 – Summary of material properties for blind test of micro-modelling

| Material | Symbol | Description | Value | COV | Reference |
|---|---|---|---|---|---|
| **Brick** | E | Elastic Modulus | 6,095 MPa | 0.29 | [10] |
| | $f_t$ | Tensile strength | 3.48 MPa | 0.42 | [14] |
| | $f_{c0}$ | Compressive elastic limit | 7.0 MPa | | [10] |
| | $F_{cp}$ | Peak compressive strength | 23.99 MPa | 0.33 | [6] |
| | $e_p$ | Compressive strain at peak strength | 0.0065 | 0.34 | [10] |
| **Mortar** | E | Elastic Modulus | 545 MPa | 0.30 | [10] |
| | $f_t$ | Tensile strength | 0.68 MPa | 0.13 | [6] |
| | $f_{c0}$ | Compressive elastic limit | 1.0 MPa | | [10] |
| | $F_{cp}$ | Peak compressive strength | 3.1 MPa | 0.22 | [10] |
| | $e_p$ | Compressive strain at peak strength | 0.0087 | 0.38 | [10] |



 



Material properties employed for the blind testing are summarized in Table 1. The simplified micro-modelling approach uses the same material for the brick and the mortar and it requires five different main parameters for the characterization of the monotonic behavior. Other parameters including Poisson ratio and the fracture energy are not included in the table. A Poisson ratio of 0.17 is used for the mortar based on experimental tests on 1:6 mortar in literature and a Poisson ratio of 0.09 is used for the brick [11]. A tensile fracture energy of 0.015 N/mm and a compressive fracture energy of 5.0 N/mm is used [12][13].
It can be seen from Figure 5 that the result of the blind prediction does not accurately capture the lateral force displacement characteristics shown by the experimental curve. The wall is considered "stocky" due to its aspect ratio of 1:2. This results in the wall "failing in shear with no flexural cracking". The experiment shows that the first crack is a stair-step diagonal crack indicated by (1) in Figure 3.
The simplified micro-model assuming blind-prediction properties has a sliding shear crack at the bottom left of the wall, shown in Figure 4b. Figure 4a shows the principal stresses obtained from the model.
A possible reason for the micro-model not accurately capturing this failure mechanism is due to the lack of boundary elements between the mortar and the bricks that prevent the possibility to capture the stress and damage distribution shown by the experimental test (see Section 2).

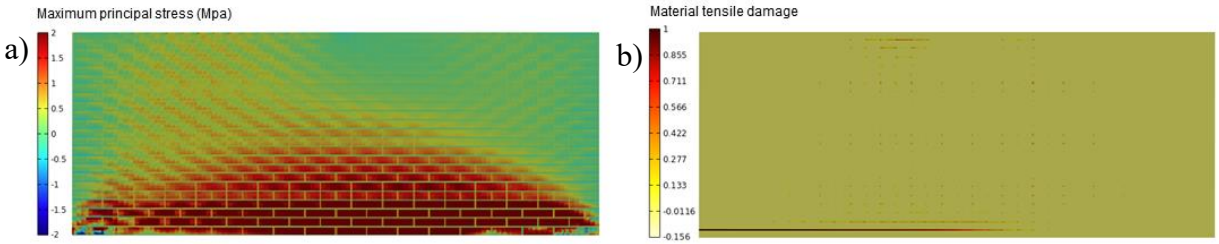


Figure 4. Results of blind test using micro-modelling a) Tensile principal stresses b) Material tensile damage

### 3.1 Material property adjustments

A possible reason for the blind test not exhibiting the same failure mechanism as the experimental tests could be due to the inconsistency in the results of the material tests. This is shown due to the relatively high coefficient of variation (COV) shown in the literature studies selected for the blind prediction.
To identify the sensitivity of each different material property on the pushover response of the wall an adjustment strategy is adopted where each parameter in Table 1 is adjusted within the standard deviation from literature ($\pm\sigma$) based on the coefficient of variation (COV) provided in [10]. Each adjustment is completed one at a time and is shown in Figure 5.
Figure 5 shows the experimental curve, the blind prediction and a series of adjusted curves. Each of these curves has the same material properties as the blind prediction except one of the material properties which has been adjusted by one $\sigma$ . When adjusting the tensile strength of each material the value is increased by $\sigma$, so the pushover has a greater peak strength. It can be seen from Figure 5 that the pushover is not very sensitive to varying the tensile strength and subsequently the pushover curves hold the same form. The elastic modulus of each material is reduced. They are reduced to help reduce initial lateral stiffness of the model to better match the experimental curve. It can be seen from Figure 5 that the reduction in the elastic modulus did result in better matching of the initial stiffness. The strain at which the peak stress occurs is increased in both materials within their experimental variability. This is done to try and increase the displacement at which the peak load occurs in the pushover. The pushover is not particularly sensitive to the adjustment of the strain value. Finally, the peak compressive stress is increased in an attempt to increase the peak lateral load of the pushover. Also in this case, the pushover is not particularly sensitive the change in peak compressive strength. The micro-modelling curves are stopped at a displacement of 2mm as the softening of the materials caused convergence issues at higher displacement.



 



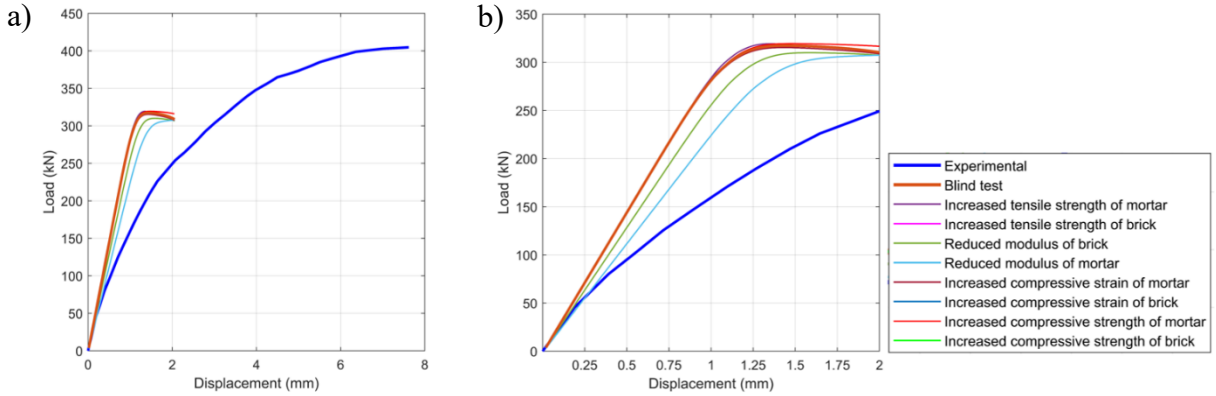


Figure 5. Comparison of blind test and the material property adjustments for the micro-modelling against the experimental data (a) Complete experimental curve compared with numerical micro-model curves (b)micro-model force-displacement results up to 2mm compared with the first portion of experimental curve

## 4 Meso-modelling

Meso-models idealise the brick-mortar combination as a continuum and therefore material properties of masonry can be used for its implementation. As part of the experimental study a prism was formed of five bricks which were capped at both ends as to maintain contact. Three of these prisms were tested in a universal compression testing machine, giving an average compression strength of 5.52 MPa with a COV of 5.5% [6]. The experimental work did not give any other material properties for the assembled masonry and therefore the masonry properties are taken from Kaushik et al [10] as to maintain consistency with the blind prediction presented in Section 3 and as the mortar and brick combination have similar properties to those used in the experimental study [6]. The tensile strength of the masonry is assumed to be equal to the tensile strength of the mortar in the micro modelling as this is considered to be the limiting factor in the tensile failure of the masonry. The first pushover for meso-modelling is attempted using a blind prediction. The material employed for the continuum in OpenSees and implemented in STKO is TC3D (i.e. the same material model used for bricks and mortar in Section 3). A summary of the key material properties for the blind test is given in Table 2. There is no COV given for the compressive elastic limit, as the source considered (i.e. [10]) does not provide a variability measure.

Table 2 – Summary of Material properties for blind test of meso-modelling

| Material | Symbol | Description | Value | COV | Reference |
|---|---|---|---|---|---|
| **Masonry Continuum** | E | Elastic Modulus | 1795 MPa | 0.24 | [10] |
| | $f_t$ | Tensile strength | 0.68 MPa | 0.13 | [6] |
| | $f_{c0}$ | Compressive elastic limit | 7.0 MPa | | [10] |
| | $F_{cp}$ | Peak compressive strength | 20.8 MPa | 0.24 | [10] |
| | $e_p$ | Compressive strain at peak strength | 0.0065 | 0.43 | [10] |

The geometry of the experimental wall is implemented into the OpenSees meso-model using STKO. The wall is modelled using a mesh of four node quad elements. An extremely stiff element is implemented directly above the masonry wall as to evenly distribute the vertical loads as well as the horizontal displacement.
Figure 6b shows the comparison of the lateral force-displacement curve for the blind meso-model and the experimental results. It can be seen that the meso-model does not start to soften until significantly larger displacements, otherwise the force-displacement can be considered relatively similar to the experimental result. The peak shear force applied to the wall is within 10% of that of the experimental results. Figure 6a



 

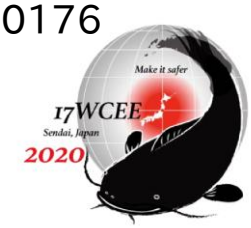



shows the material tensile damage and it can be seen that the wall fails due to diagonal shear cracking similar to the trend shown in Figure 3. This most likely explains why it better captures the response relative to the micro-model.

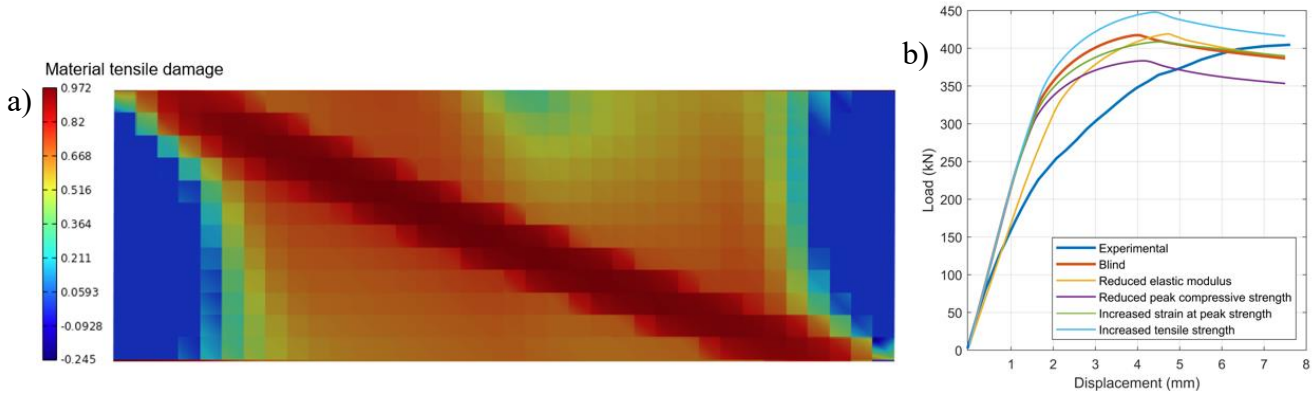


Figure 6. Results of blind test with meso-model (a) Material tensile damage (b) Comparison of blind test and the material property adjustments for the meso-modelling against the experimental data

### 4.1 Material property adjustments

The blind prediction of the meso-modelling captures the failure mechanism but still does not match the experimental curve. A possible reason is that there is significant variability in the material properties of the masonry material. To identify if a better characterization of the experimental curve can be obtained, each of the material properties is adjusted. Each of the material properties is individually adjusted within its variability ($\pm\sigma$) to enable an assessment of whether this shows better matching with the experimental. For each material property both $+\sigma$ and $-\sigma$ is run and a visual inspection is used to assess which result gives better matching with the experimental curve. The results are shown in Figure 6b. The best matching occurs with the experimental curve when the elastic modulus is reduced as the strain at which the peak load occurs is increased.

## 5. Conclusions

This study modelled the force-displacement response of an unreinforced masonry wall using both simplified micro modelling and meso-modelling. These models were implemented into OpenSees using the Scientific Toolkit for OpenSees and the materials were modelled using the tension and compression damage material model developed by Petracca and Camata. The materials properties were taken from the experimental study where possible and when the material properties were not provided, they were obtained from a study by Kaushik et al. where solid clay bricks, various mortars and masonry prisms were tested under uniaxial compression. These material properties were used to run a "blind test" for both the micro and meso-models. The material properties were then shifted one-by-one within their experimental variability using the coefficient of variation provided in the literature studies to identify the ruling parameters for a better numerical-to-experimental matching.

The simplified micro-model did not exhibit a load-displacement relationship similar to the experimental results, furthermore it is shown from the material damage and maximum principal stresses that the failure mechanism is different from the experimental failure mechanism. The simplified micro-model fails due to a sliding shear crack whereas the experimental tests fails due to a series of consecutive diagonal shear cracks. The individual material properties were then adjusted and it was shown that this did not significantly improve the matching with the experimental data.

The meso-model had a load-displacement response that was much closer to that of the experimental study and furthermore the material damage showed the meso-model failed due to diagonal shear cracking replicating more closely the failure mechanism shown by the experimental results. The individual material properties were then adjusted and it was observed that reducing the elastic modulus resulted in slightly better matching with the experimental test.



 

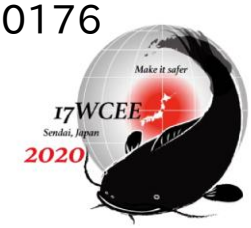



The preliminary assessment of the two modelling strategies emphasises how a blind testing can be more satisfactory using a meso-model approach. On the other hand, more extensive numerical-to-experimental comparisons are needed considering campaigns with richer material information to further confirm the above observation.

## Acknowledgements

This research is funded by the Leverhulme Trust (RPG-2017-006, GENESIS project). The first author acknowledges the support of EPSRC (EP/R513179/1).

## References

[1] Lourenço P B (2010). Recent advances in masonry modelling: micromodelling and homogenisation. *Multiscale modeling in solid mechanics: computational approaches* (pp. 251-294).
[2] Lourenco P B, Rots J G, Blaauwendraad J (1995). Two approaches for the analysis of masonry structures: micro and macro-modeling. *HERON*, **40**(4), 1995.
[3] Rodrigues H, Varum H, Costa A (2010). Simplified macro-model for infill masonry panels. *Journal of Earthquake Engineering*, **14**(3), 390-416.
[4] Kamal O A, Hamdy G A, El-Salakawy T S (2014). Nonlinear analysis of historic and contemporary vaulted masonry assemblages. *HBRC Journal*, **10**(3), 235-246.
[5] Pantò B, Caliò I, Lourenço P (2017). Seismic safety evaluation of reinforced concrete masonry infilled frames using macro modelling approach. *Bulletin of Earthquake Engineering*, **15**(9), 3871-3895.
[6] Abrams D, Shah N (1992). Cyclic Load Testing of Unreinforced Masonry Walls. *Advanced Construction Technology Center.* University at Urbana, Illinois.
[7] De Luca F, Giordano N, Gryc H, Hulme L, McCarthy C, Sanderson V, Sextos A (2019). Nepalese School Building Stock and Implications on Seismic Vulnerability Assessment. *ICEE-PDRP 2019 2nd International Conference on Earthquake Engineering and Post Disaster Reconstruction Planning*, 25-27 April, Bhaktapur, Nepal
[8] Novelli V., Ngoma I., Kloukinas P., Kafodya, I., De Risi R., Macdonald J., & Goda K. (2019). Seismic Vulnerability Assessment of Non-Engineered masonry buildings in Malawi. *COMPDYN 2019 7th ECOMAS Thematic Conference on Computational Methods in Structural Dynamics and Earthquake Engineering* 24–26 June, Crete, Greece.
[9] Petracca M, Camata G (2019). A Mixed Implicit-Explicti Tension-Compression Plastic-Damage Model. *ASDEA Software Technology*, Pescara, Italy.
[10] Kaushik H, Rai D, Jain S (2007). Stress-Strain Characteristics of Clay Brick Masonry under Uniaxial Compression. *Journal of Materials in Civil Engineering*, **19**(9), pp.728-739.
[11] Nwofor T C (2012). Experimental determination of the mechanical properties of clay brick masonry. *Canadian Journal on Environmental, Construction and Civil Engineering*, **3**(3), 127-145.
[12] Chaimoon K, Attard M M (2007). Modeling of unreinforced masonry walls under shear and compression. *Engineering structures*, **29**(9), 2056-2068.
[13] Van Zijl G P (2004). Modeling masonry shear-compression: role of dilatancy highlighted. *Journal of engineering mechanics*, **130**(11), 1289-1296.
[14] Lourenço P, Almeida J, Barros J (2005). Experimental investigation of bricks under uniaxial tensile testing. *Journal of the British Masonry Society Masonry International*, **18**(1).



 